

# A Novel Design Approach to X-Band Minkowski Reflectarray Antennas using the Full-Wave EM Simulation-based Complete Neural Model with a Hybrid GA-NM Algorithm

Filiz GÜNEŞ<sup>1</sup>, Salih DEMİREL<sup>1</sup>, Selahattin NESİL<sup>1,2</sup>

<sup>1</sup>Dept. of Electronics and Communication Engineering, Yıldız Technical University, 34220 Esenler, Istanbul, Turkey

<sup>2</sup>Informatics and Information Security Research Center (BILGEM), TUBITAK, Gebze, Turkey

gunes@yildiz.edu.tr, salihd@yildiz.edu.tr, selahattin.nesil@tubitak.gov.tr

**Abstract.** *In this work, a novel multi-objective design optimization procedure is presented for the Minkowski Reflectarray RA s using a complete 3-D CST Microwave Studio MWS- based Multilayer Perceptron Neural Network MLP NN model including the substrate constant  $\epsilon_r$  with a hybrid Genetic GA and Nelder-Mead NM algorithm. The MLP NN model provides an accurate and fast model and establishes the reflection phase of a unit Minkowski RA element as a continuous function within the input domain including the substrate  $1 \leq \epsilon_r \leq 6$ ;  $0.5 \text{ mm} \leq h \leq 3 \text{ mm}$  in the frequency between  $8 \text{ GHz} \leq f \leq 12 \text{ GHz}$ . This design procedure enables a designer to obtain not only the most optimum Minkowski RA design all throughout the X- band, at the same time the optimum Minkowski RAs on the selected substrates. Moreover a design of a fully optimized X-band  $15 \times 15$  Minkowski RA antenna is given as a worked example together with the tolerance analysis and its performance is also compared with those of the optimized RA s on the selected traditional substrates. Finally it may be concluded that the presented robust and systematic multi-objective design procedure is conveniently applied to the Microstrip Reflectarray RAs constructed from the advanced patches.*

## Keywords

Genetic and Nelder–Mead algorithms, Minkowski, Multilayered Perceptron Neural Network (MLP), optimization, tolerance analysis, reflectarray antenna.

## 1. Introduction

Microstrip reflectarray antennas RAs are able to provide equivalent performance of a traditional parabolic reflector, but their simple structures with low profiles, light weights and no need of any complicated feeding networks are advantageous. This can be achieved designing each RA element to reflect the incident wave independently with a phase compensation proportional to the distance from the

phase centre of the feed-horn to form a pencil beam in a specified direction  $\theta_0, \varphi_0$  as is well-known from the classical array theory. Thus, “phasing” is very important process in designing reflectarray. In literature different approaches of compensating the phase of each element have been proposed, however phasing method using the variable size patches is preferable choice in many designs due to its simplicity [1], [2].

Since it is simple to manufacture the microstrip RA on a single layer, in order to satisfy requirements as the capability to radiate a shaped beam or multi-beams, or also to enhance the frequency behavior and bandwidth, the advanced patch configurations are necessary to be worked out in which the structure has a lot of degrees of freedom and all concur to the performances of the whole antenna. The management of different parameters and the need of satisfying requirements that could be also in opposite each other could however make the design of a reflectarray quite complex. Therefore first of all for a computationally efficient optimization process, an accurate and rapid model for the reflection phase of a unit element is needed to be established as a continuous function in the input domain of the patch geometry and substrate variables. Then it could be convenient to carry this model out adopting a hybrid “global + local” search method to find the best solution among all the possible solutions.

This article puts forward a robust methodology for design optimization of the microstrip RAs. Our research group has worked with the Minkowski shape [3-6] which is from the 1st iteration of fractals and the Minkowski radiator is shown to have an optimum phasing characteristic with the fairly large linear region and easy fabrication [7]. The systematic design optimization procedure presented in this article can briefly be summarized in the following stages:

(i) The first stage is to build a rapid and accurate model for the reactive impedance behavior of a Minkowski radiator. For this purpose, a MLP NN is optimized by the Levenberg-Marquardt algorithm using the data sets obtained by the 3-D CST-based simulation of a Minkowski

radiator placed at the end of a standard X-band waveguide. Thus the reflection phase of a unit Minkowski element is established independently as a continuous function within the input domain of the element geometry  $m$ ,  $n$  and substrate parameters  $\epsilon_r$ ,  $h$  in the X-band;

(ii) In the second stage, a hybrid GA–NM algorithm is used to select the most proper phasing characteristic for the calibration characteristic as the one having slower gradient with respect to the geometry  $n$  and substrate  $\epsilon_r$ ,  $h$  parameters and the wider range to achieve a wider operational bandwidth and smaller susceptibility to manufacturing errors using the MLP NN model. In addition to optimization process, the sensitivity and yield analyses are applied as tolerance analysis of optimized parameters.

(iii) The third stage is the implementation stage. In this stage the reflectarray having  $15 \times 15$  Minkowski interspaced by half-wavelengths at 11 GHz is designed reversing the MLP NN model. In this stage, the different designs are made corresponding to the fully or partially optimized antenna parameters;

(iv) In the final stage, performance analyses of the designed RAs are made employing the 3-D Computer Simulation Technology Microwave Studio (CST MWS) simulations and compared and discussed.

The organization of the paper is as follows: The next section is devoted to the discretization of the 5-dimensional Minkowski space of  $(m, n, \epsilon_r, h, f)$  to obtain the training and validation data for MLP NN. In the third section gain and bandwidth optimization will be presented using the hybrid combination of Genetic and Nelder-Mead algorithms with respect to the input variables. In addition, the sensitivity and yield analyses are performed for the tolerance analysis in order to specify the tolerance limits of optimized design parameters. Design and performance analysis of the Minkowski RA s with the optimized or non-optimized antenna parameters will be taken place in the fourth and fifth sections, respectively. Finally the conclusions end the paper.

## 2. Reflection Phase Characterization of a Minkowski Radiator

### 2.1 Minkowski Space

In the design of microstrip RA, the shape and geometry selection of the RA element is the crucial part as well as the substrate properties chosen. In this work, the geometry of radiating element has been proposed to be a resonant element shape for a periodic RA structure, which is a first fractal type, so called Minkowski shape. Fig. 1(a) and (b) show the geometrical representation of Minkowski shape patch element and the H-wall waveguide simulator, respectively.

The relationship between the Minkowski parameters is formulated as:

$$n = \frac{s}{m/3}, \quad 0 \leq n \leq 1 \quad (1)$$

In (1),  $s$  is the indentation and  $m$  is the width of the patch, respectively and  $n$  refers the indentation ratio. The reflection response of unit cell and phase of reflected wave are generated by the 3D CST MWS-based analysis implemented to the H-wall waveguide simulator which is shown in Fig. 1(b). The top and bottom surfaces of the H-wall waveguide simulator are perfectly electric conducting walls, while the right and left walls are perfectly magnetic field walls [2]. The vertically polarized incoming waves will be incident normally onto the element at the end of the waveguide at the broadside direction and then scattered back also at the broadside direction with a set of amplitude and phase information.

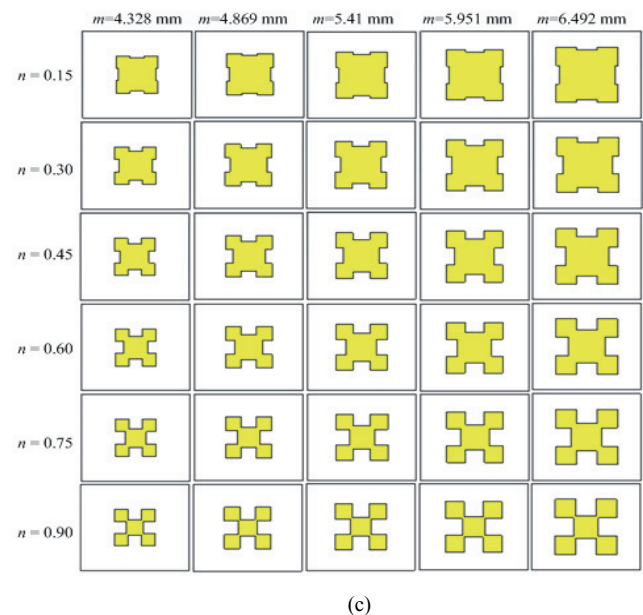
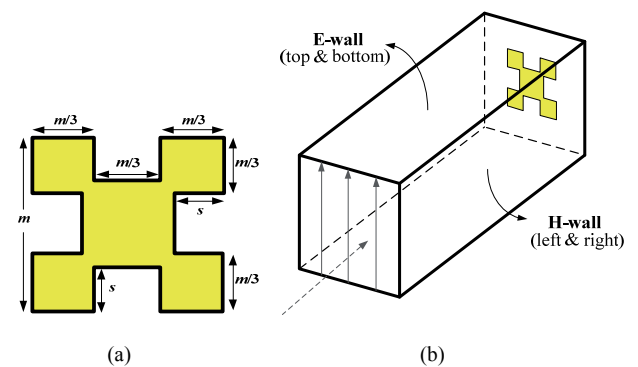


Fig. 1. For a Minkowski radiator: (a) Geometrical representation. (b) The H-wall waveguide simulator. (c) The  $n_s \times m_s = 6 \times 5 = 30$  sampling Minkowski matrix [6].

The 5-dimensional discretized Minkowski space of  $(m, n, \epsilon_r, h, f)$  are constructed by totally 5400 samples to be used in the training and validation of the MLP NN model using the H-Wall waveguide simulator analyzed by 3-D CST MWS as follows:

The operation bandwidth of 8-12 GHz is swept as the intervals of 1 GHz and the resulted number of the sample frequencies is  $f_s = 5$ . Then, Minkowski sampling matrix (Fig. 1c) is generated as  $n_s \times m_s$  for each sampled substrate properties  $(\epsilon_r, h)$  at each sampling frequency where  $n_s = 6$  and  $m_s = 5$  are the number of samples for the indentation factor and patch width within the ranges of  $0.15 \leq n \leq 0.90$  and  $m \pm (\Delta m/m)_{\max} = m \pm 20\%$  where  $m$  is the resonant length at 11 GHz, respectively. Simultaneously the substrate thickness  $h$  is sampled as the intervals of 0.5 mm between them  $0.5 \text{ mm} \leq h \leq 3 \text{ mm}$  and the total number of the thickness sampling is  $h_s = 6$ . In addition, dielectric permittivity of substrate  $\epsilon_r$  is totally sampled  $\epsilon_s = 6$  times between  $1 \leq \epsilon_r \leq 6$ . Thus, the entire Minkowski space is discretized totally into the  $\epsilon_s \times f_s \times h_s \times m_s \times n_s = 5400$  Minkowski configurations.

### 2.2 The MLPNN Black-Box Modeling

The black-box model of a Minkowski radiator is depicted in Fig. 2a where the MLPNN is employed for the generalization process which is already given in Fig. 2b. The MLP NN has the two hidden layers each of which consists of 10 neurons activated by the tangential sigmoid function. The input  $\vec{x}$  and output  $\vec{y}$  vectors are 5- and 1-dimensional, respectively and can be expressed as

$$\vec{x} = [m \ n \ \epsilon_r \ h \ f]^t, \quad \vec{y} = [\varphi_{11}]^t = \varphi_{11}(\vec{x}, \vec{w}) \quad (2)$$

where  $\vec{w}$  is the weighting vector of the MLP NN given in Fig. 2b and the output function  $\varphi_{11}(\vec{x}, \vec{w})$  can be built using the MLPNN theory [8].  $\vec{w}$  is determined by the optimization with the following mean-squared error function over the training data using the Levenberg- Marquardt algorithm [9]:

$$E = \sum_{k \in T_r} (\varphi_{11k} - d_k)^2 \quad (3)$$

where  $T_r$  is an index set of the training data which consists of 3240  $(\vec{x}, \varphi_{11})$  data pairs corresponding to the patch lengths of 4.328 mm, 5.41 mm and 6.491 mm, the rest 2160  $(\vec{x}, \varphi_{11})$  data pairs are used to validate the MLP NN model. The Linear Regression scattering plots for the training and the validation process are given in Figs. 3a and 3b, respectively with their Mean Squared Error MSEs

Some examples of modeling performances are depicted in Figs. 4a, b, c where the constructed phasing characteristics are compared with their targets. Furthermore Fig. 5a and 5b gives the three dimensional view of the reflection phase variations with the patch width  $m$  and the relative permittivity of substrate value  $\epsilon_r$ 's for the constructed and targeted data at the fixed conditions of  $h = 1.5 \text{ mm}$ ,  $n = 0.6$ ,  $f = 11 \text{ GHz}$ . Thus, it can be inferred that the MLP NN model works very well in generalization of the 5400  $(\vec{x}, \varphi_{11})$  data pairs to the entire domains to obtain the continuous Minkowski reflection phasing func-

tion  $\varphi_{11}(\vec{x})$ . In the next section, this  $\varphi_{11}(\vec{x})$  function will be used directly to determine the phase calibration characteristic and later it will be reversed to synthesize the Minkowski RA in the Memetic optimization procedure.

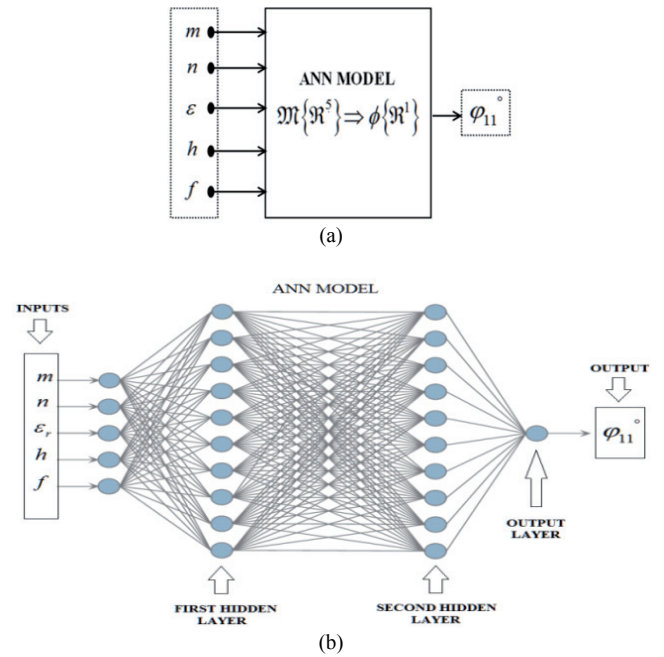


Fig. 2. For a Minkowski radiator: (a) Black-box model, (b) the MLP NN structure.

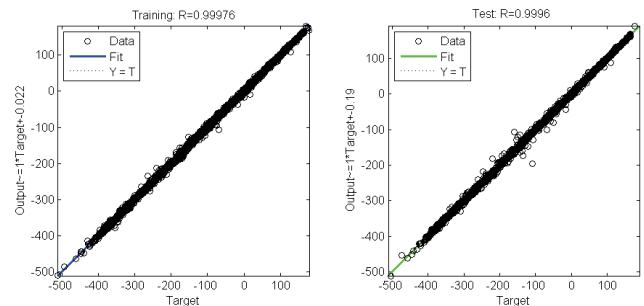
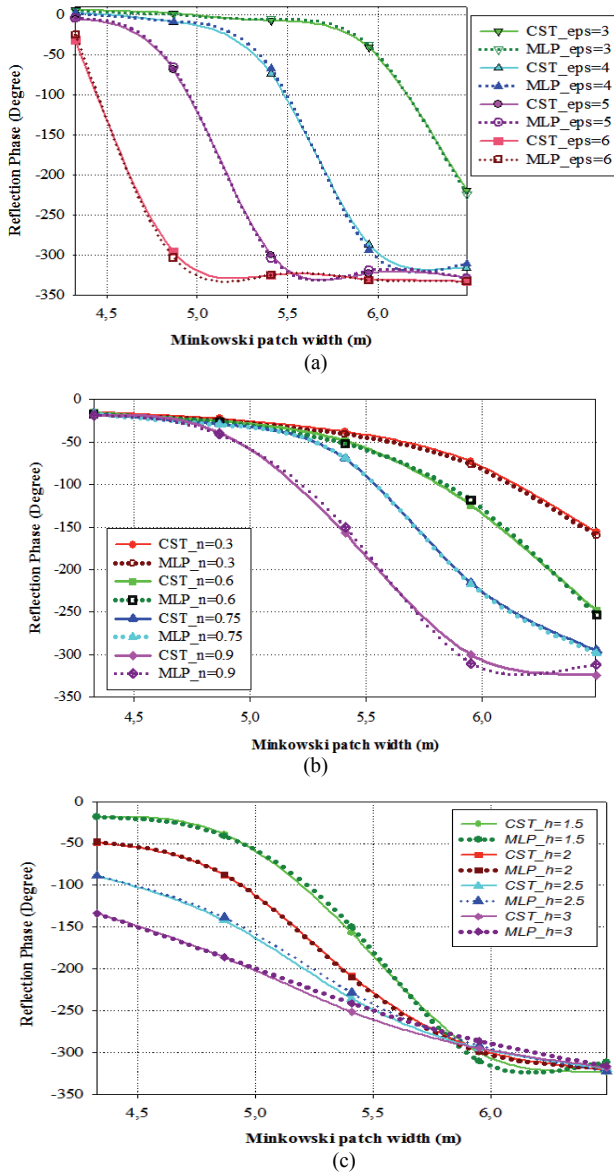


Fig. 3. Linear Regression scattering plots for the complete Minkowski MLP NN model: (a) Training (MSE Error =  $9.9564 \times 10^{-5}$ ). (b) Validation (MSE Error =  $1.7264 \times 10^{-4}$ ).

Table 1 gives the comparison of the reconstructed data for TACONIC RF 35 built by the ANN model with the experimental and simulation results made by Zubir [7].

Patch size change (%)	Results of this study		Results of ZUBIR et al. [7]	
	Target data (°)	Reconstructed data (°)	Target data (°)	Measured data (°)
-20	-24,228	-23,776	6.4797	-16.5188
-10	-50,994	-53,195	-19.0891	-39.6383
0	-176,368	-170,462	-178.9874	-196.3713
+10	-292,906	-295,782	-284.6809	-290.3985
+20	-317,745	-309,813	-304.348	-323.4595

Tab. 1. Comparison for reconstructed data by ANN with the simulated data for conditions  $f = 11 \text{ GHz}$ ,  $n = 0.75$ ,  $h = 1.524 \text{ mm}$ ,  $\epsilon_r = 3.54$  (Taconic RF-35) and the measured results in [7].



**Fig. 4.** Reflection phase characteristics for (a)  $h = 1$  mm,  $n = 0.60$ ,  $f = 11$  GHz; taking dielectric constant  $\epsilon_r$  as parameter; (b)  $\epsilon_r = 3$ ,  $h = 1.5$  mm,  $f = 11$  GHz and indentation ratio  $n$  is parameter; (c)  $\epsilon_r = 3$ ,  $n = 0.90$ ,  $f = 11$  GHz and substrate thickness  $h$  is parameter.

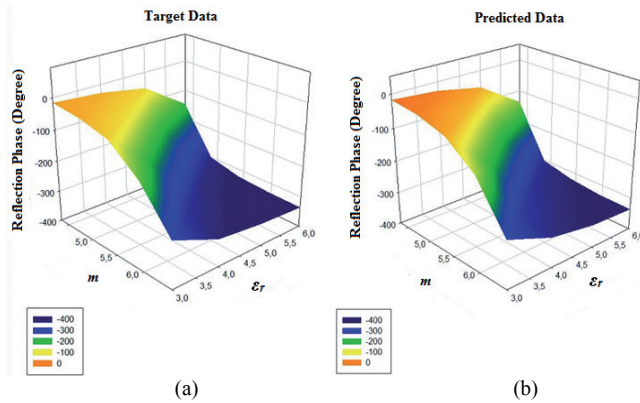


**Fig. 5.** Three dimensional reflection phase variations versus the patch width  $m$  and the relative permittivity  $\epsilon_r$  for the fixed conditions of  $h = 1.5$  mm,  $n = 0.6$ ,  $f = 11$  GHz for (a) target and (b) constructed data.

### 3. Phase Calibration Characteristic

#### 3.1 Objective Function

In this section, a multi-objective optimization procedure is established where the phase calibration characteristic is selected among the phasing characteristics obtained in the previous section as the one having the slower gradient and the wider range with respect to the indentation of patch  $n$  and substrate ( $\epsilon_r$ ,  $h$ ) to achieve the wider band and smaller susceptibility to the manufacturing errors. Thus, this objective can be expressed as the sum of the three ingredients as follows:

$$Objective = \text{Min} \left\{ \sum_{n,h,\epsilon_r} \mathcal{G}_i(n,h,\epsilon_r) \right\} \quad (4)$$

with the following objective  $\mathcal{G}_i$  at the frequency  $f_i$ :

$$\mathcal{G}_i = \left\{ \sum_{\substack{\epsilon_r=1 \\ \Delta\epsilon_r=0.01}}^6 \sum_{\substack{h=0.5\text{mm} \\ \Delta h=0.01\text{mm}}}^{3\text{mm}} \sum_{\substack{n=0.15 \\ \Delta n=0.01}}^{0.9} W_1 \cdot \epsilon_1(f_i) + W_2 \cdot \epsilon_2(f_i) + W_3 \cdot \epsilon_3(f_i) \right\} \quad (5)$$

where,

$$\epsilon_1 = e^{-\left( \frac{\varphi_{\max} - \varphi_{\min}}{360} \right)}, \quad (6a)$$

$$\epsilon_2 = |\varphi_{\max} - \varphi_{\text{center}}| - |\varphi_{\min} - \varphi_{\text{center}}|, \quad (6b)$$

$$\epsilon_3 = 1 - \left( \frac{\Delta\varphi_{\text{center}}}{\Delta m_{\text{center}}} \right). \quad (6c)$$

In (6a,b,c),  $\varphi_{\max}$ ,  $\varphi_{\min}$  and  $\varphi_{\text{center}}$  are the reflection phase values at  $m_{\max}$ ,  $m_{\min}$  and  $m_{\text{center}}$  for a certain  $(n, \epsilon_r, h)$  set, respectively at the  $f_i$  where  $\ell, c, u$  stand for the lower, center and the upper frequencies. In the optimization process, operation frequency range is defined as follows:  $f_\ell = 10$  GHz,  $f_c = 11$  GHz,  $f_u = 12$  GHz. In (6a), the phase difference between  $\varphi_{\max}$  and  $\varphi_{\min}$  is normalized by dividing 360 and in (6b) ( $\Delta\varphi_{\text{center}} / \Delta m_{\text{center}}$ ) is the gradient of the phasing characteristic at the point of  $(\varphi_{\text{center}}, m_{\text{center}})$  which is aimed at to be equal to unity corresponding to optimum angle  $\pi/4$ . Thus,  $\epsilon_1$  is used to maximize the phase range while  $\epsilon_2, \epsilon_3$  provide the centralization of the characteristic with the slope equal to the unity. All weighting coefficients ( $W_1, W_2$ , and  $W_3$ ) in (5) have been taken as unity. Optimization process is completed as soon as the iteration number has reached to its maximum value or the predefined cost value. In our case, the optimization ends when the cost value reaches to 0.4353 with the optimized values of all the weighting coefficients.

#### 3.2 The Memetic Algorithm: Hybrid GA-NM Algorithm

A Memetic algorithm MA is essentially a combination of a population-based global optimization algorithm with a local search [10]. Recently, Memetic algorithms

consisting of the hybrid GA-NM and Bacterial Swarm Optimization BSO - NM algorithms are successfully implemented to designs of the low-noise microwave amplifier and bow-tie antennas in [11] and [12], respectively.

In this work, a Genetic Algorithm GA is used as a population-based global optimizer and a simple local search algorithm called Nelder-Mead NM [13] is employed along with the GA to reduce the cost of the solution at each iteration of the optimization procedure (Fig. 6).

The GA uses the evolution operations which are the crossover, mutation and recombination together with the concept of fitness. The population is built by the chromosomes as the solution candidates, binary encoded randomly varied as 0 and 1. The objective function corresponding to each chromosome is evaluated, then chromosomes are ranked according to their fitness's and the least fit ones are discarded and the remaining chromosomes are paired at randomly selected crossover points. In order to prevent the solution from being trapped into the local minima, mutation process is applied by transforming a small percentage of the bits in the chromosome from 0 to 1 or vice versa. The mutation process per iteration is applied for 1% of the chromosomes.

The MA used in our work can be briefly described through the following abstract description [12]:

```

Begin
Population Initialization
LocalSearch
Evaluation
Repeat
Crossover
Recombination
Mutation
Local Search
Evaluation
Selection
Until termination criterion is satisfied
Return best solution
End
    
```

Here, the initial populations are usually generated in a random or controlled manner and then the evolution of these populations is carried out by the genetic operators such as crossover, mutation and recombination. Local search is utilized to reduce the cost of the resulted solution from the global optimization.

In our GA-NM application, the MATLAB [9] is used for the Memetic algorithm with the selection of stochastic uniform operators consisting of a population (chromosome) of 60, number of generation of 900, crossover probability of 0.8 (or crossover fraction for reproduction is 0.8), and mutation probability of 0.001. Mutation function is constraint dependent. Crossover function is scattered. Migration direction is just forward numbered 0.2. The convergence occurs very quickly typically within the 30 iterations shortening 5 times as compared with the 60 iterations GA process, which takes 1 min and 12 s and 5 min and 41 s with Core i7 CPU, 1.60 GHz Processor, 4 GB RAM depending on the initialization values. A typical convergence curve is given in Fig. 6.

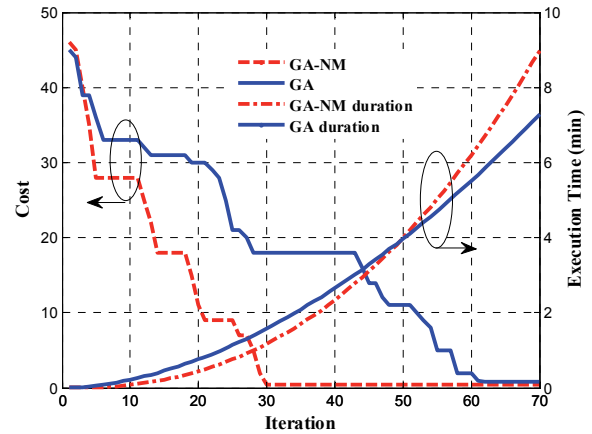


Fig. 6. Convergence performances of the genetic and memetic optimization.

According to the objective function given (4) and (5), parameters of the optimum Minkowski RA within X-band are found as  $\epsilon_r = 3.1694$ ,  $h_{opt} = 1.7916$  mm,  $n_{opt} = 0.8438$  and the corresponding reflection characteristics and values are given in Fig. 7 and Tab. 2, respectively as compared with the square radiator's reflection properties. Radiation analysis of the  $15 \times 15$  variable-size Minkowski RA with half-wave spacing at resonant frequency of 11 GHz and comparison with the designs both non-optimized and optimized on some traditional substrates are given in the following sections.

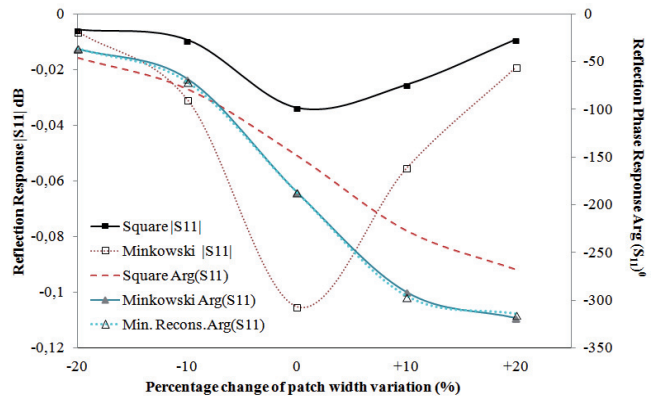


Fig. 7. Reflection characteristics of the Optimum Minkowski Reflectarray element with the parameters of  $n_{opt} = 0.8438$ ,  $\epsilon_{ropt} = 3.164$  and  $h_{opt} = 1.7916$  mm at  $f = 11$  GHz as compared with the square patch's values having the same resonance frequency.

Patch width (mm)	Square patch (Resonant size=6.09 mm)		Minkowski patch (Resonant size=5.41 mm)		
	S <sub>11</sub>   (dB)	Target Arg(S <sub>11</sub> ) (°)	S <sub>11</sub>   (dB)	Target Arg(S <sub>11</sub> ) (°)	Recons. Arg(S <sub>11</sub> ) (°)
-20	-0,00575	-46,4841112	-0,0064	-37,016407	-35,9411
-10	-0,00945	-79,192581	-0,03085	-68,385344	-70,9368
0	-0,03373	-148,82782	-0,10519	-187,0838	-186,72
10	-0,02543	-227,4055	-0,05529	-291,59329	-295,5879
20	-0,00919	-268,14059	-0,01901	-318,6572	-314,4403

Tab. 2. 3-D EM simulated reflection phases of the Optimum Minkowski Reflectarray element and constructed phases by the complete ANN response as compared with the square patch at  $f = 11$  GHz.

### 3.3 Tolerance Analysis of the Optimized Parameters

The design parameters may usually change in a certain tolerance region during the manufacturing process. Thus it is of interest to which percentage the design specifications are fulfilled. Thus the yield analysis is applied to compute an expected tolerance as percentage. In the implementation of yield analysis, variations in the design parameters are assumed to be small so that the linearization via the sensitivity analysis can be valid. For this reason a yield analysis can only be applied after a successful run of the sensitivity analysis. In the sensitivity analysis, the derivatives of output function (in our case it is reflection phase) with respect to geometric and/or material design parameters can be calculated without re-meshing the example. The first derivative of the network function with respect to a design parameter can be calculated with the information of the nominal value in a small neighborhood of that nominal value. Also the sensitivity information is used for a more efficient optimization.

In this study, sensitivity analysis is applied to the optimum dielectric constant  $\epsilon_{ropt} = 3.164$  by rounding up the other parameters, as  $n_{opt} = 0.85$ ,  $h_{opt} = 1.8$  mm. Then the yield analysis is applied to the results of the sensitivity analysis for the three values of the standard deviation belonging to the dielectric constant. The graphics for these results are shown in Fig. 8.

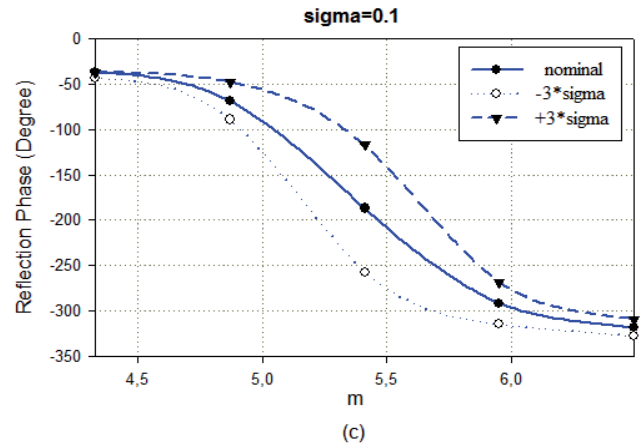
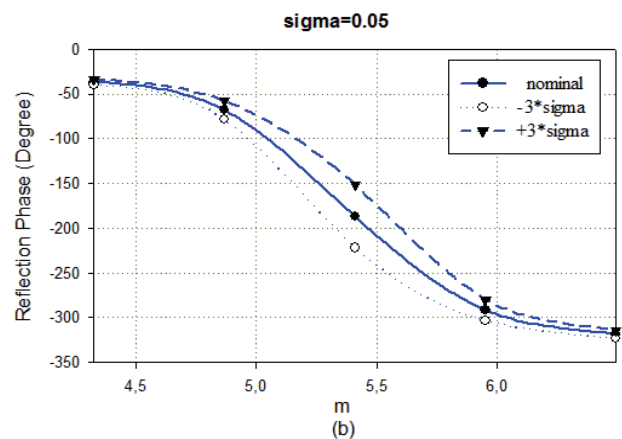
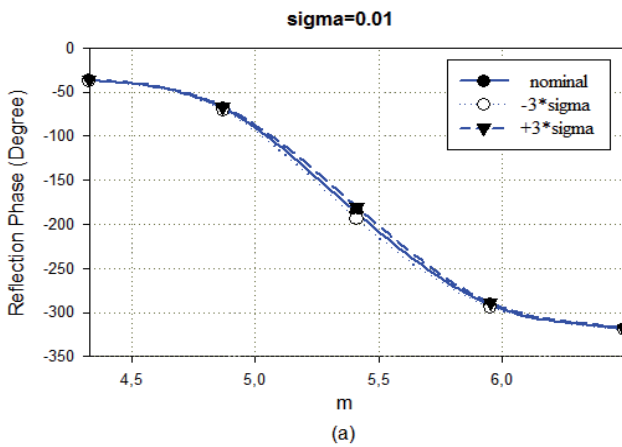


Fig. 8. Sensitivity analysis results for the optimum dielectric constant for the standard deviation (sigma) values: (a)  $\sigma = 0.01$ , (b)  $\sigma = 0.05$ , (c)  $\sigma = 0.1$  at  $f = 11$  GHz.

As is seen from Fig. 8, the best tolerance is at the nominal design parameter value with a lower and upper bound ( $-3 \cdot \sigma$ ,  $+3 \cdot \sigma$ ) of the dielectric permittivity when the sigma is equal to 0.01. The upper and lower bound indicate the worst case limits of the tolerance for the dielectric property of substrate. The substrate that has closest specifications to the optimized parameters had been searched, and the two commercially available substrates which are Rogers RO3003 and RO4232 has been found. As is seen from Fig. 9, RO4232 is the fittest substrate as commercially available for our optimized parameter result.

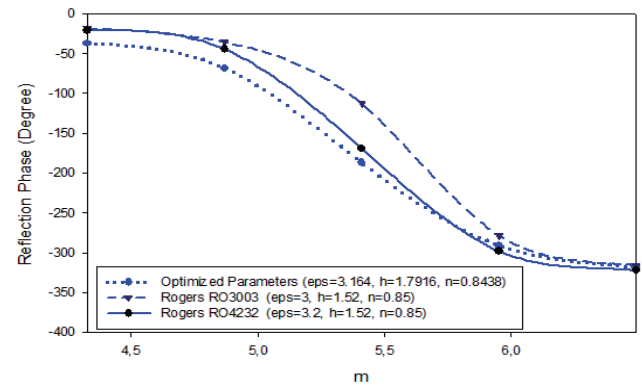


Fig. 9. Comparison of the reflection phase responses for unit cell element designed with optimized parameters and two equivalent commercially available substrates.

## 4. Design of the Variable-Size RA

### 4.1 Phase Compensation

In this work, the  $15 \times 15$  variable-sizes Minkowski RA with half-wave spacing at resonant frequency of 11 GHz are designed. The radiation analysis has been generated using available full-wave simulation tool of CST MWS. In the phase compensation unit, a coordinate system has been used to determine the progressive phase distribution on the microstrip reflectarray surface of  $M \times N$  arbitrarily spaced

patches with a centered focal point that will produce a pencil beam in a direction of normal to the surface [8]. Thus, the required phase to compensate path difference  $\Delta R(x)$  for a reflectarray element can be given as a function of its radial distance  $x$  to the center and the operation frequency  $f$  as follows:

$$\begin{aligned} \varphi(x, f) &= -\beta(\Delta R_{\max} - \Delta R(x)) \\ &= -\frac{2\pi f}{c} F \left( \sqrt{1 + (D/F)^2} / 4 - \sqrt{1 + (x/F)^2} \right) \end{aligned} \quad (7)$$

where the minus sign expresses delay,  $c$  is the velocity of light. In (7)  $D$  and  $F$  are the diameter and the focal length of the feed to the array center, respectively. Quadrature symmetry characteristic of the phase compensation with respect to the element position for the  $15 \times 15$  reflectarray where frequency is considered as the parameter and  $F/D$  is taken as 0.8.

### 4.2 Determination of Size of Each Radiator

Size of each radiator is determined to meet the necessary compensation phase using the phase calibration char-

acteristic. For this purpose, the established ANN model is reversed by inputting optimum values corresponding the phase calibration characteristic and while input  $m$  changes itself using the adaptable size  $\Delta m$ 's which get exponentially smaller with an adaptation parameter  $\tau$  as decreasing the squared error as given in Fig. 10 [6].

## 5. Implementation

In the implementation stage, all the radiation performance analyses are made using 3-D CST Microwave Studio.

The fully optimized X-band Minkowski reflectarray antenna with the parameters  $\epsilon_{r\text{opt}} = 3.1694$ ,  $h_{\text{opt}} = 1.7916$  mm,  $n_{\text{opt}} = 0.8438$  is designed using the general design procedure (Fig. 10) and its realized gain patterns at the frequencies 10.5 GHz, 11 GHz and 11.9 GHz are given in Fig. 11a. Furthermore for the purpose of comparison, the realized gain patterns of an arbitrary non-optimized RA antenna with the parameters of  $\epsilon_r = 2.2$ ,  $h = 1.5$  mm,  $n = 0.90$  at the same frequencies are obtained with the same

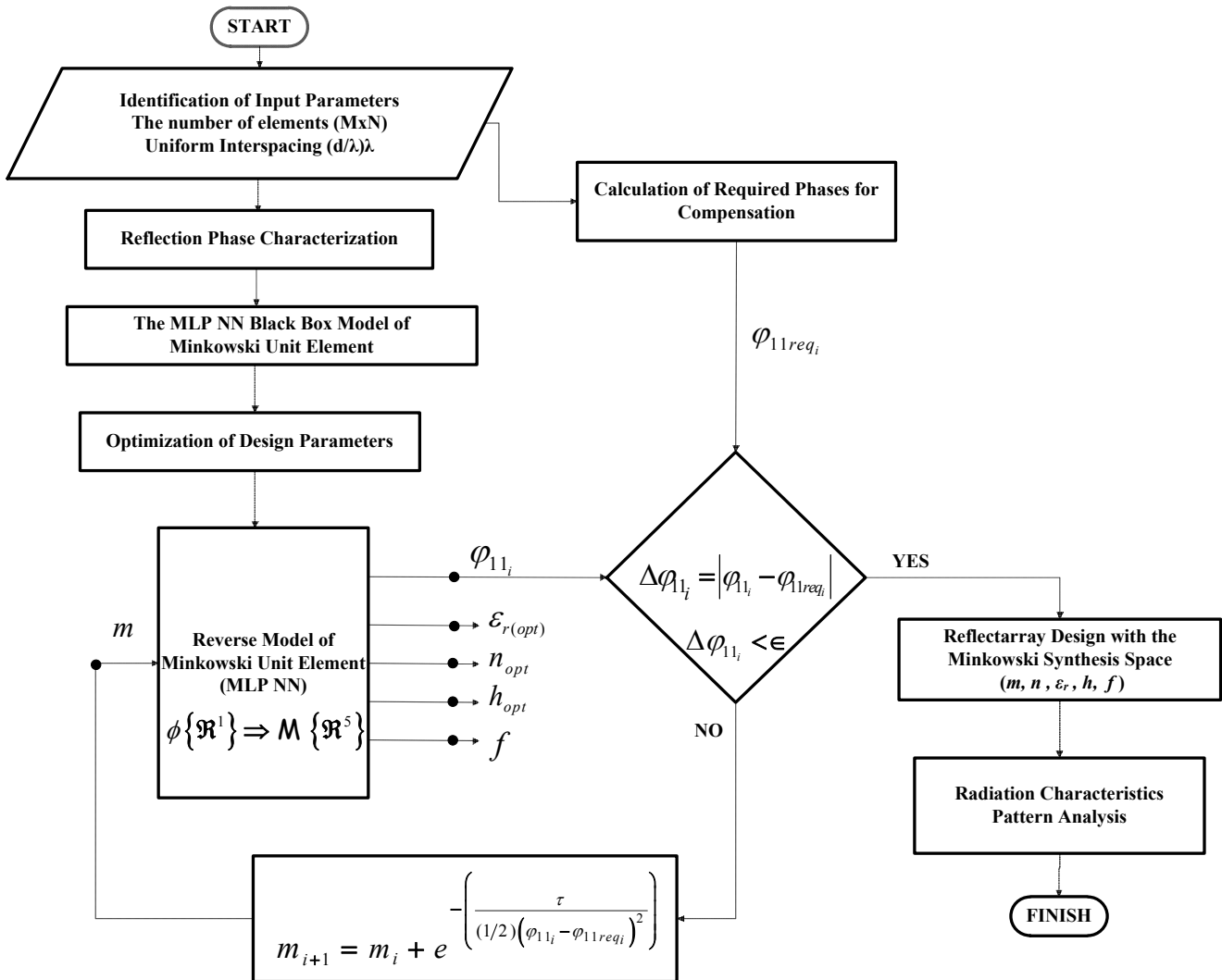


Fig. 10. Design flow diagramme for the optimum reflectarray antenna.

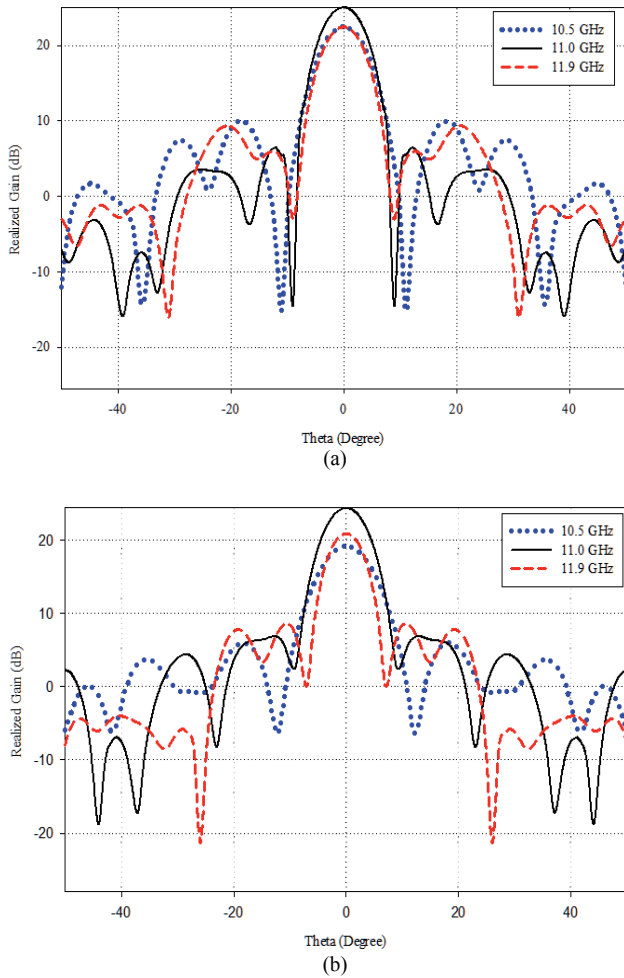


Fig. 11. (a) Fully optimized RA with  $\epsilon_{r,opt} = 3.1694$ ,  $h_{opt} = 1.7916$  mm,  $n_{opt} = 0.8438$ ; (b) Non-optimized reflectarray with  $\epsilon_r = 2.2$ ,  $h = 1.5$  mm,  $n = 0.90$ .

Antenna	Freq. (GHz)	Realized gain (dB)	Side lobe level (dB)	Angular width (3dB) (deg)
Optimized reflectarray $\epsilon_{r,opt} = 3.1694$ , $h_{opt} = 1.7916$ mm, $n_{opt} = 0.8438$	10.5	22.5	-12.5	7.9
	11	25	-18.6	7.4
	11.9	22.5	-13.2	7.1
Non-optimized reflectarray $\epsilon_r = 2.2$ , $h = 1.5$ mm, $n = 0.90$	10.5	19.2	-13.2	8.8
	11	24.4	-17.5	7.5
	11.9	21	-12.4	6.3

Tab. 3. Performance comparison of the fully optimized reflectarray with a non-optimized reflectarray.

procedure (Fig. 10) and depicted in Fig. 11b and the compared performance values take place in Tab. 3. In order to examine the influence of dielectric property optimization, the gain variation with respect to the frequency are obtained with the same optimized indentation ratio  $n_{opt} = 0.8438$  and thickness  $h_{opt} = 1.7916$  mm, but on some traditional substrates which are Taconic RF-35 with  $\epsilon_r = 3.5$ , Taconic TRF41 with  $\epsilon_r = 4.1$ , Rogers TMM4 with  $\epsilon_r = 4.5$  and depicted in Fig. 12. The performance values corre-

sponding to Fig. 12 take place in Tab. 4. Fig. 13 depicts the gain versus frequency variations of the optimized RAs designed on the dielectric  $\epsilon_{r,opt} = 3.1694$  and the traditional substrates in Fig 12. The performance values belonging to Fig. 13 are given in Tab. 5.

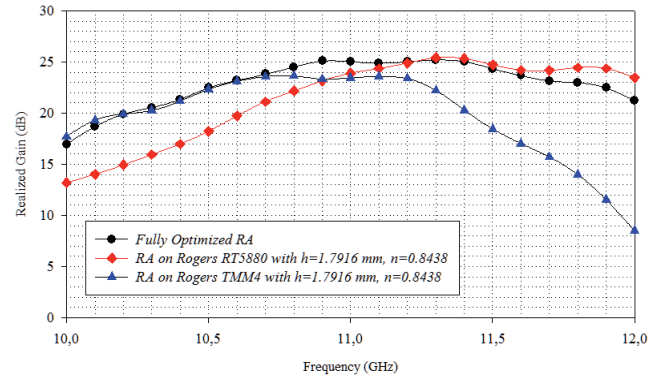


Fig. 12. Realized gain versus frequency graphs for the fully optimized RA and the other RAs on the different substrates with the optimized parameters  $n_{opt}$ ,  $h_{opt}$ .

Freq. (GHz)	Realized gain (dB)		
	Fully optimized RA $\epsilon_{r,opt} = 3.1694$ , $h_{opt} = 1.7916$ mm, $n_{opt} = 0.8438$	Rogers RT5880 $\epsilon_r = 2.2$ , $h_{opt} = 1.7916$ mm, $n_{opt} = 0.8438$	Rogers TMM4 $\epsilon_r = 4.5$ , $h_{opt} = 1.7916$ mm, $n_{opt} = 0.8438$
10	17	13.2	17.7
10.5	22.5	18.2	22.3
11	25	23.9	23.5
11.5	24.3	24.7	18.5
12	21.2	23.5	8.5

Tab. 4. Comparison of the fully optimized RA and the other RAs designed on the different substrates with the same optimized parameters  $n_{opt}$ ,  $h_{opt}$ .

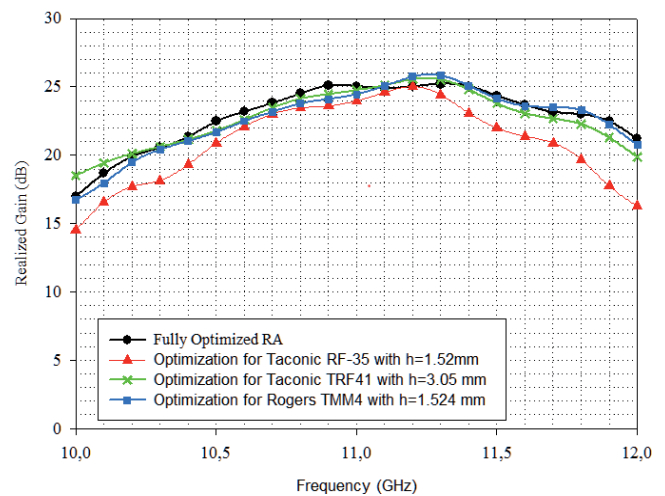


Fig. 13. Realized gain versus frequency variations for the comparison of fully optimized RA with only patch geometry  $n_{opt}$  optimized RAs on the given dielectric permittivity  $\epsilon_r$  and substrate thickness  $h$ .

Freq. (GHz)	Realized Gain (dB)			
	Optimized reflectarray $\epsilon_{r,opt}=3.1694$ , $h_{opt}=1.7916$ mm, $n_{opt}=0.8438$	Taconic RF-35 $\epsilon_r=3.5$ , $h=1.52$ mm, $n_{opt}=0.7848$	Taconic TRF41 $\epsilon_r=4.1$ , $h=3.05$ mm, $n_{opt}=0.6212$	Rogers TMM4 $\epsilon_r=4.5$ , $h=1.524$ mm, $n_{opt}=0.3604$
10	17	14.5	18.5	16.7
10.5	22.5	20.9	21.8	21.7
11	25	24	24.8	24.5
11.5	24.3	22	23.8	24.1
12	21.2	16.3	19.9	20.7

**Tab. 5.** Comparison of the fully optimized RA and RAs with the optimized Minkowski shapes on the traditional substrates.

## 6. Conclusions

Doubtlessly, Microstrip Reflectarrays are of prime importance in today’s antenna technology, since they combine the advantages of both the printed phased arrays and parabolic reflectors to create a new generation of high gain antennas.

In this paper, a robust and systematic method is put forward to be used in the design and analysis of a Minkowski reflectarray. The most important and critical stage of a reflectarray design is the design optimization of its element. Therefore, firstly a complete, accurate and fast MLP ANN model of a Minkowski patch radiator is built based on the 3-D CST Microwave Studio MWS that takes into account all the main factors influencing the performance of the Minkowski RA. When the outputs of performed MLP ANN model and 3-D simulations are compared, it is verified that the MLP is very accurate and fast solution method to construct the highly nonlinear phasing characteristics within the continuous domain of the geometrical and substrate parameters of the RA element and frequency. All the stages of building the MLP ANN model and its utilization in design of a Minkowski RA are given in details as a general systematic method that can be applied to the differently shaped patch radiators.

In the second stage, the overall parameters of Minkowski RA including dielectric permittivity of the substrate  $\epsilon_r$  are optimized for an optimum linear phasing range of an ultra- wideband RA in the X- band by applying a standard novel evolutionary hybrid combination of Global Genetic GA and local Nelder-Mead NM algorithms.

In addition to optimization process, the sensitivity and yield analyses are performed for the tolerance analysis in order to specify the tolerance limits of optimized design parameters and the commercially available substrate options which are compatible with our optimized design parameters. The optimum dielectric permittivity tolerance limits are qualified rounding up the values of the optimum substrate thickness  $h_{opt}$  and indentation ratio of Minkowski microstrip patch  $n_{opt}$  for the three characteristic values of the standard deviation. Thus this tolerance analysis results

in the limits of design parameters and the proper commercial available dielectric substrate as Rogers RO4232.

In the final stage, a fully-optimized 15×15 Minkowski RA is designed as a worked example. Thus, its radiation characteristics are analyzed based on the 3-D CST Microwave Studio MWS and graphically represented, then compared with the performances of the non-optimized and the partially-optimized Minkowski RAs.

It may be concluded that the presented method can be considered as a robust and systematic method for the design and analysis of a microstrip reflectarray antenna built by the advanced patches.

## References

- [1] POZAR, D. M., METZLER, T. A. Analysis of a reflectarray antenna using microstrip patches of variable size. *Electronics Letters*, 1993, vol. 27, p. 657–658.
- [2] HUANG, J., ENCINAR, J. A. *Reflectarray Antennas*. Wiley-IEEE Press, 2007. ISBN: 978-0470-08491-4.
- [3] NESİL, S., GÜNEŞ, F., ÖZKAYA, U. Phase characterization of a reflectarray unit cell with Minkowski shape radiating element using Multilayer Perceptron Neural Network. In *7th International Conference on Electrical and Electronics Engineering ELECO*. Dec. 2011, p. 219-222.
- [4] NESİL, S., GÜNEŞ, F., ÖZKAYA, U., TÜRETKEN, B. Generalized regression neural network based phase characterization of a reflectarray employing Minkowski element of variable size. In *URSI*. Turkey, 2011.
- [5] NESİL, S., GÜNEŞ, F., KAYA, G. Analysis and design of X-band reflectarray antenna using 3-D EM-based Artificial Neural Network model. In *IEEE International Conference on Ultra-Wideband ICUWB*. Sept. 2012, p. 532-536.
- [6] GÜNEŞ, F., NESİL, S., DEMİREL, S. Design and analysis of Minkowski reflectarray antenna using 3-D CST Microwave Studio-based Neural Network Model with Particle Swarm Optimization. *International Journal of RF and Microwave Computer-Aided Engineering*, 2013, vol. 23, p. 272–284.
- [7] ZUBIR, F., RAHIM, M. K. A., AYOP, O., WAHID, A., MAJID, H. A. Design and analysis of microstrip reflectarray antenna with Minkowski shape radiating element. *Progress in Electromagnetics Research B*, 2010, vol. 24, p. 317–331.
- [8] ZHANG, Q. J., GUPTA, K. C. *Models for RF and Microwave Components*. Neural Networks for RF and Microwave Design. Norwood (MA): Artech House, 2000.
- [9] MATLAB and Neural Networks Toolbox Release 2012b, The MathWorks, Inc., Natick, Massachusetts, United States.
- [10] KONSTANTINIDIS, A., YANG, K., CHEN, H.-H., ZHANG, Q. Energy-aware topology control for wireless sensor networks using memetic algorithms. *Elsevier Computer Communications*, 2007, vol. 30, no. 14, p. 2753–2764.
- [11] CENGİZ, Y., KILIÇ, U. Memetic optimization algorithm applied to design microwave amplifier for the specific gain value constrained by the minimum noise over the available bandwidth. *International Journal of RF and Microwave Computer-Aided Engineering*, 2010, vol. 20, p. 546–556.
- [12] MAHMOUD, K. R. Design optimization of a bow-tie antenna for 2.45 GHz RFID readers using a hybrid BSO-NM algorithm. *Progress in Electromagnetics Research*, 2010, vol. 17, p. 100-105.

- [13] NELDER, J. A., MEAD, R. A simplex method for function minimization. *Computer Journal*, 1965, vol. 7, p. 308-313.

### About Authors...

**Filiz GUNES** received her M.Sc. degree in Electronics and Communication Engineering from the Istanbul Technical University. She attained her Ph.D. degree in Communication Engineering from the Bradford University in 1979. She is currently a full professor in Yıldız Technical University. Her current research interests are in the areas of multivariable network theory, device modeling, computer-aided microwave circuit design, monolithic microwave integrated circuits, and antenna arrays.

**Salih DEMIREL** has received M.Sc. and Ph.D. degrees in Electronics and Communication Engineering from Yıldız Technical University, Istanbul, Turkey in 2006 and 2009,

respectively. He has been currently working as an Assistant Professor in the same department. His current research interests are among of microwave circuits especially optimization of microwave circuits, broadband matching circuits, device modeling, computer-aided circuit design, microwave amplifiers.

**Selahattin NESIL** was born in Afyonkarahisar, Turkey on June 27, 1980. He received the B.Sc. and M.Sc. degrees in Electronics Engineering from Fatih University, Istanbul, Turkey in 2004 and 2007, respectively. He has been a Ph.D. candidate in Electronics and Communication Engineering at Yıldız Technical University, Turkey since 2008. Now, he is working as a Chief Researcher at Informatics and Information Security Research Center (BILGEM), TUBITAK, Turkey. His research interests include reflect-array antennas, optimization systems, artificial intelligence systems, antenna theory, and design, as well as computational and applied electromagnetics.